Bipolar Resistance Switching in Fully Transparent ZnO:Mg-Based Devices

Lei Shi, Dashan Shang*, Jirong Sun, and Baogen Shen

Beijing National Laboratory for Condensed Matter Physics and Institute of Physics, Chinese Academy of Sciences, Beijing 100190, P. R. China

Received July 21, 2009; accepted August 31, 2009; published online September 18, 2009

Transparent indium–tin-oxide/ZnO:Mg/F-doped SnO_2 devices that show bipolar resistance switching have been successfully fabricated. In addition to the transmittance above 80% for visible light, the devices show a high-to-low resistance ratio greater than 2.5, an endurance more than 10^5 cycles, and a resistance retention longer than 5000 s even at the temperature of 110 °C. The field-induced resistance change can be explained based on the formation/rupture of conduction filaments, due to the migration of structural defects in electric field. The present work shows the potential application of resistive random access memory to invisible electronics.

DOI: 10.1143/APEX.2.101602

Transparent devices are important due to their potential application in invisible electronics.[1] Transparent ferroelectric capacitors,[2] p–n diodes,[3,4] and thin film transistors have been obtained.[5] However, transparent nonvolatile memory devices, which are indispensable for invisible electronics, are still lacking because of the opaqueness of silicon, which is the basic material for the silicon-based technology that holds the largest share of nonvolatile memories.

Recently, a device composed of an insulating layer sandwiched by two electrodes has been proposed, which showed reversible electric field-induced resistance switching.[6–19] Based on this effect, a technology for information memory, resistive random access memory (RRAM), can be developed. According to their dependence on bias polarity, the RRAM devices can be classified into the bipolar and unipolar ones. For the former, electric fields of different polarity are required to trigger the resistance between two definite states, while there is no polarity dependence for the latter. Up to now, a large variety of materials have been found to show the characteristics of resistance switching, such as the binary oxides NiO, TiO_2, CuO_x, ZrO_2, ZnO,[8–12] the perovskite oxides Pr(or La)$_{0.7}$Ca$_{0.3}$MnO$_3$, Cr-doped $SrZrO_3$, $SrTiO_{3-\delta}$,[13–16] and the solid electrolytes Cu_2S, Ag_2S, Cu-doped SiO_2.[17–19] Among them, ZnO is especially attractive. It is transparent for visible light (band gap > 3.1 eV), and could be used for the design of transparent nonvolatile memory device. Recently, Seo *et al.* obtained a transparent RRAM (TRRAM) device by sandwiching a ZnO film between two transparent electrodes.[20] This device shows an unipolar character. To explain the resistance change, the formation and rupture of conduction filaments in ZnO, under the impact of electric field and Joule heating, respectively, have been proposed. Considering the improved transparency in Mg-doped ZnO due to band gap expansion,[21] in this work, we reported on a TRRAM device composed of Mg-doped ZnO and two oxide electrodes. In addition to excellent transparency, the device shows an electric polarity dependent resistance switching. This effect can be explained based on the formation/rupture of conduction filaments due to the migration of structural defects in electric field.

Ceramic target with the nominal composition of $Zn_{0.8}Mg_{0.2}O$ (ZnO:Mg) was prepared by mixing ZnO and MgO powders in the atomic ratio of Zn : Mg = 8 : 2, grinding and then sintering the resultant mixture at 1000 °C for 10 h in air. Commercial glass capped by a ~150 nm thick F-doped SnO_2 (FTO) layer, which has a transmittance above 95%, was used as substrate and simultaneously bottom electrode. ZnO:Mg films of ~300 nm were deposited on the glass substrates by the pulsed laser deposition (PLD) technique, using a KrF laser ($\lambda = 248$ nm) with a fluence of 7 J/cm^2 and a repetition rate of 5 Hz. The substrate temperature is 400 °C and the oxygen pressure is 10 Pa during the deposition.

Square-shaped indium–tin-oxide (ITO) top-electrodes with different sizes between 50×50 and $400 \times 400\,\mu m^2$ (defined by the photolithography and lift-off technique) were prepared by the PLD at the temperature of 130 °C and the oxygen pressure of 0.5 Pa. In_2O_3/SnO_2(9 : 1) alloy was selected as the target. The resultant samples were characterized by X-ray diffraction (XRD; Rigaku D/MAX-2400), atomic force morphology (AFM; Seiko Instruments SPA400), and photoemission spectroscopy (XPS; VG Scientific ESCALAB-5) with the Al Kα line (1486.6 eV). Current–voltage (I–V) characteristics and resistance switching of the samples were measured by a Keithley SourceMeter 2601. The electric bias directing from the top to the bottom electrode is defined to be positive.

Figures 1(a) and 1(b) present the photographs of the ITO/ZnO:Mg/FTO/glass. The device is fully transparent, as shown by the clear image of the underlying logo. The transmission spectrum, measured by an UV–visible spectrophotometer, indicates the transmittance above 80% in the wavelength region 450–800 nm [Fig. 1(c)].

Figure 2 shows the XRD, AFM, and XPS results of the ZnO:Mg film. The weak diffraction peaks indicate the polycrystalline characters of the ZnO:Mg film. The obviously high (002) peak suggests a (002) preferential orientation of the ZnO:Mg grains. The grains are fairly uniform as shown by the AFM image in Fig. 2(b). The peaks of Zn $2p_{1/2}$ and $2p_{2/3}$ at the binding energy of 1045.8 and 1022.4 eV, respectively, Mg 2p at 50.5 eV, and O 1s at 530.2 eV indicate that Zn/Mg is fully oxidized and exists as Zn^{2+}/Mg^{2+}. The atomic ratio of Zn to Mg, estimated from integrated intensity values, after a proper consideration of corresponding sensitivity, is ~2 : 1, lower than that of the target. The lower Zn content in the film could be due to the volatilization loss during the sample preparation.

Figure 3(a) presents the typical I–V characteristics of the ITO/ZnO:Mg/FTO device (electrode size = 100×100 μm^2), measured by sweeping voltage, at a speed of 50 mV/s,

*E-mail address: shang_da_shan@163.com

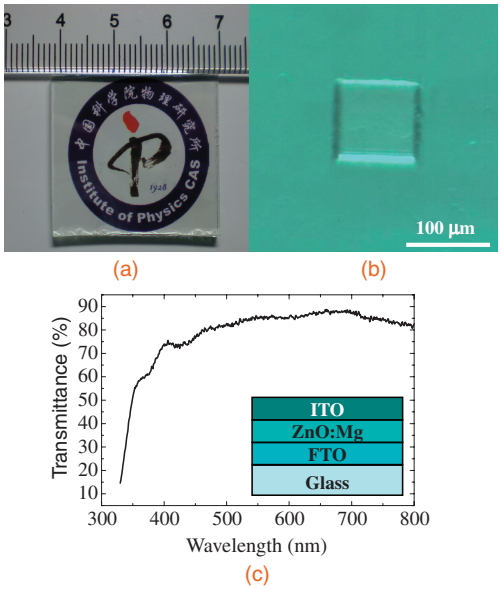

Fig. 1. (a) A photograph of the ITO/ZnO:Mg/FTO/glass device placed on a background logo. (b) A close view of the TRRAM unit with only one top electrode. Since the focus s on the device surface, the logo below the device cannot be seen in this case. (c) Optical transmission spectrum of the ITO/ZnO:Mg/FTO/glass device. Inset in (c) is a schematic diagram of the TTRAM structure.

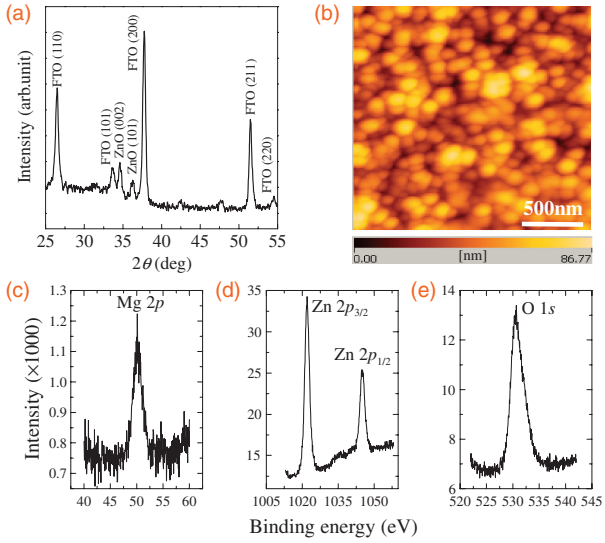

Fig. 2. (a) XRD pattern of the ZnO:Mg film on FTO/glass. (b) Topographic of the ZnO:Mg film measured by AFM. (c)–(e) Respective XPS spectra of the Mg 2p, Zn 2p, and O 1s lines.

in the sequence of $0 \rightarrow 3 \rightarrow 0 \rightarrow -3 \rightarrow 0$ V. The inset plot in Fig. 3(a) shows the electrode setting of the device. With the increase of the positive bias, a sudden change in resistance occurs at $V_{T1} = 2.8$ V, indicating the switching to a low resistance state (LRS). The sample remains in the LRS for subsequent bias descending, and the backward transition to a high resistance state (HRS) occurs only after the $0 \rightarrow -3 \rightarrow 0$ V cycling, as signified by the occurrence of the anticlockwise I–V hysteresis. It should be noted that the resistance of the HRS is lower than that of the initial resistance state (IRS), which indicates the difference of these two states. Further cycling in the range $-3 \rightarrow 3$ V yields repeatable I–V characteristics, with a reduction in the critical

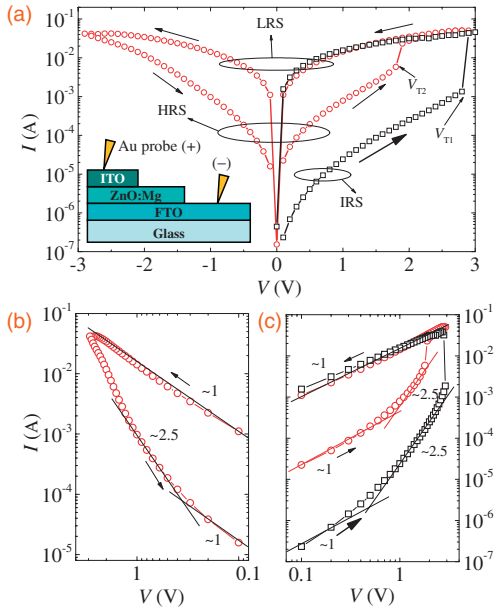

Fig. 3. (a) Semilogarithmic I–V characteristics of the ITO/ZnO:Mg/FTO device (electrode size = 100 × 100 μm^2). Inset in (a) shows a schematic diagram of the measurement. (b,c) Log–log plot of the I–V curves in the positive and negative bias regions, respectively. Arrows indicate the sweeping directions.

voltage for the HRS → LRS transition ($V_{T2} = 1.8$ V). We also measured the I–V characteristics without changing bias polarity and observed no oscillation between the LRS and the HRS. This is different from the ITO/ZnO/ITO device, for which a resistance alternation can be produced by repeatedly applying biases with the same polarity.[20]

Figure 3(c) presents a log–log plot of the I–V curves. With the increase of bias voltage, both the IRS and HRS exhibit first a $I \propto V$ then a $I \propto V^{2.5}$ relationship. This is the typical behavior of trap-controlled space-charge-limited conduction (SCLC).[22] The ohmic conduction dominates the transport behavior when the density of injected carriers in the ZnO:Mg film is lower than that of the thermally generated ones. Otherwise, the transport is controlled by the carrier trapping process. In contrast, the LRS exhibits a simple ohmic behavior. The abrupt change from the SCLC of the HRS to the ohmic conduction of the LRS could be ascribed to the occurrence of metallic filaments as noted later in this paper.

The resistance switching triggered by electric pulses was further studied. As shown in Fig. 4(a), the resistance of the sample, measured under 0.1 V between two neighboring pulses, oscillates between the LRS and HRS under the impact of alternative electric pulses of 3 and −3 V (pulse width = 1 s). The resistance shows a high-to-low ratio of at least 2.5 and little degradation after 10^5 cycles, indicating the good endurance of the device. Both the HRS and LRS are quite stable up to at least 110 °C [Fig. 4(b)]. These results show the reliability of the TRRAM as nonvolatile memory device.

It is instructive to note the electrode size independence of the LRS resistance [Fig. 4(c)]. This result indicates, as well established, a filament-dominated conduction in the LRS.[23] In contrast, the resistance shows a monotonic decrease as electrode size grows for the IRS and a weak dependence on electrode area for the HRS. The latter may suggest an inhomogeneous conduction as will be discussed later.

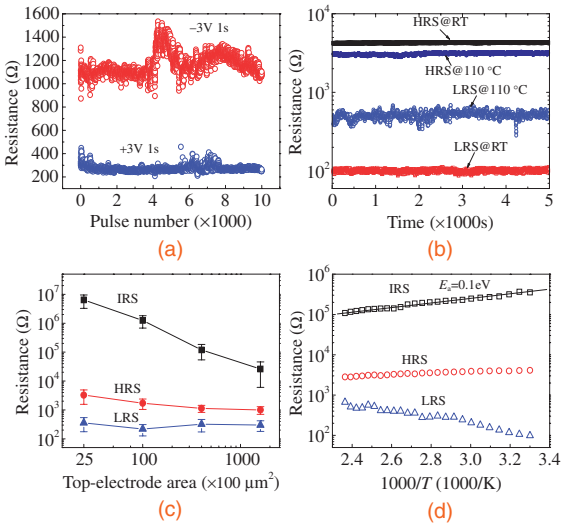

Fig. 4. (a) Electric pulse-induced resistance switching of the ITO/ZnO:Mg/FTO device. (b) Retention property of the resistance state at the room temperature and 110 °C. (c,d) Dependence of resistance on the size of the ITO electrode and temperature.

Further information on conduction mechanism can be obtained from the temperature dependence of the resistance. As shown in Fig. 4(d), the conduction of the IRS shows a semiconductorlike behavior and the resistance of the IRS decreases exponentially with the increase of temperature following the relation $R = R_0 \exp(E_a/kT)$, where R_0 is a constant independent of temperature, $E_a \approx 0.1$ eV is the activation energy for charge carriers, k the Boltzmann's constant, and T the temperature. Different from the IRS, the resistance of the LRS increases upon warming. It implies the occurrence of metallic conduction during the LRS transition. Since there are no signatures of diffusion and percolation of metallic elements in our devices, the metallic transport could be ascribed to a field-induced arrangement of structural defects, resembling the situation in the $SrTiO_{3-\delta}$ single crystal.[16] The resistance–temperature relation of the HRS locates between those of the IRS and LRS, manifesting a close relation with these two states.

Based on the above results, a scenario for the bipolar resistance switching in the ITO/ZnO:Mg/FTO device can be drawn. Under low external biases ($V < V_{T1}$), structural defects such as oxygen vacancies, metallic defects, and gain boundaries, which are inevitable for the polycrystalline ZnO:Mg films, act as trap centers for charge carriers and cause the trap-controlled SCLC transport behavior. Grain boundaries and dislocations make it easy for the point defects, probably oxygen vacancy, to diffuse in a high electric field, resulting in percolating conduction filaments, thus the LRS transition.[6] This is similar to that occurred in the ITO/ZnO/ITO, Pt/ZnO/Pt, and Pt/ZnO:Mg/Pt devices, which show the unipolar resistance switching.[20,24,25] However, the experimental data show that the LRS of our sample is affected only by reverse electric fields. Therefore, the simple thermal effects produced by Joule heating as the origin for the LRS → HRS transition can be excluded, even if it exists. The polarity dependence of the resistance switching in the ITO/ZnO:Mg/FTO device may have a close relation with the asymmetric electrode structure. A possible reason for the rupture of the conduction filaments in the present device is the annihilation of the oxygen vacancies near the ITO/ZnO:Mg interface by the oxygen diffusion from ITO that works as an oxygen reservoir. This situation is similar to that occurred in the TiN/ZnO/Pt device.[26] In addition to oxygen diffusion, the migration of indium ion in the ZnO:Mg film, the former can be easily dissolved into the latter as donor,[27] under the driving of electric field is also possible, yielding the polarity-dependent resistance switching. In fact, Yang *et al.* have reported a bipolar resistance switching of Ag/ZnO:Mn/Pt, due to the formation and rupture of nanoscale Ag bridges in the ZnO:Mn films under the biases with different polarity.[28] The metallic filaments may not be destroyed completely in the HRS → LRS process and the remaining fragments cause the inhomogenous conduction in the ZnO:Mg film. As a consequence, the resistance of the HRS is much lower than that of the IRS and weakly dependent on the electrode area and temperature. It is obvious that further experiments are required to clarify the detailed mechanisms for the resistance switching in the ZnO-based devices.

In summary, fully transparent devices exhibiting a bipolar resistance switching have been fabricated by sandwiching the ZnO:Mg films between the ITO and FTO electrodes on a glass substrate. In addition to excellently repeatable resistance switching, the samples exhibit excellent endurance and retention. A possible mechanism for the resistance change has been proposed based on the formation and rupture of conduction filaments due to the migration of structural defects in electric field. The present work shows the great potential of the TRRAM in invisible electronics.

Acknowledgments This work has been supported by the National Basic Research of China, the National Natural Science Foundation of China, the Knowledge Innovation Project of the Chinese Academy of Science, the Beijing Municipal Nature Science Foundation.

1) J. F. Wager: Science **300** (2003) 1245.
2) K. K. Uprety *et al.*: J. Appl. Phys. **102** (2007) 084107.
3) A. Kudo *et al.*: Appl. Phys. Lett. **75** (1999) 2851.
4) H. Yanagi *et al.*: Solid State Commun. **121** (2001) 15.
5) E. M. C. Fortunato *et al.*: Adv. Mater. **17** (2005) 590.
6) R. Waser and M. Aono: Nat. Mater. **6** (2007) 833.
7) J. J. Yang *et al.*: Nat. Nanotechnol. **3** (2008) 429.
8) S. Seo *et al.*: Appl. Phys. Lett. **85** (2004) 5655.
9) B. J. Choi *et al.*: J. Appl. Phys. **98** (2005) 033715.
10) A. Chen *et al.*: Appl. Phys. Lett. **92** (2008) 013503.
11) X. Wu *et al.*: Appl. Phys. Lett. **90** (2007) 183507.
12) M. Villafuerte *et al.*: Appl. Phys. Lett. **90** (2007) 052105.
13) S. Q. Liu *et al.*: Appl. Phys. Lett. **76** (2000) 2749.
14) D. S. Shang *et al.*: J. Mater. Res. **23** (2008) 302.
15) A. Beck *et al.*: Appl. Phys. Lett. **77** (2000) 139.
16) K. Szot *et al.*: Nat. Mater. **5** (2006) 312.
17) T. Sakamoto *et al.*: Appl. Phys. Lett. **91** (2007) 092110.
18) K. Terabe *et al.*: Nature (London) **433** (2005) 47.
19) C. Schindler *et al.*: IEEE Trans. Nanotechnol. **5** (2006) 535.
20) J. W. Seo *et al.*: Appl. Phys. Lett. **93** (2008) 223505.
21) S. Choopun *et al.*: Appl. Phys. Lett. **80** (2002) 1529.
22) K. C. Kao and W. Huang: *Electrical Transport in Solids* (Pergamon, Oxford, U.K., 1981) p. 150.
23) I. H. Inoue *et al.*: Phys. Rev. B **77** (2008) 035105.
24) W. Y. Chang *et al.*: Appl. Phys. Lett. **92** (2008) 022110.
25) X. M. Chen *et al.*: Appl. Phys. Lett. **93** (2008) 093501.
26) N. Xu *et al.*: Appl. Phys. Lett. **92** (2008) 232112.
27) Ü. Özgür *et al.*: J. Appl. Phys. **98** (2005) 041301.
28) Y. C. Yang *et al.*: Nano Lett. **9** (2009) 1636.